Theoretical Study of Transition-Metal Adhesion on Doped Al_2O_3

Pere Alemany,† R. Samuel Boorse, James M. Burlitch, and Roald Hoffmann*

Department of Chemistry and Material Science Center, Cornell University, Ithaca, New York 14853-1301

Received October 9, 1993. Revised Manuscript Received January 11, 1993

The effect of doping α-Al_2O_3 with an electron acceptor (Cr^{3+}) on adhesion to first row transition metals is studied by tight-binding extended Hückel band structure calculations. Charge transfer from the metal to the partially filled t_{2g} levels of the dopant enhance the metal–ceramic interface strength. A predicted side effect is the weakening of the Cr–O bonds in the ceramic, leading to possible adhesive failure in the first layers of the oxide phase. The adhesive energy is predicted to increase with dopant concentration, although not showing a simple linear dependence.

Adhesion between metals and ceramics plays a critical role in many materials applications. Good adhesive properties are especially important in microelectronics or in the formation of protective coats for metals. One clear example of this is the poor adhesion of copper to aluminum oxide. One of the problems faced in the industrial use of these composite materials is the fragile nature of the interfaces formed by compounds with interesting properties. Enhancing adhesion of metals to ceramics would open a wide range of new applications for these composite materials.

One way to modify the adhesive properties of a metal–ceramic couple is to include dopants in one or both components. These impurities may change the chemical bonding at the surface of the materials and modify adhesion. In this paper we will analyze the effect on adhesion of Cr^{3+} ions as dopants in α-Al_2O_3, when interfaces are formed between this material and transition metals. Both the changes in the electronic structure and the dependence of adhesion energy on dopant concentration will be addressed.

Adhesion of Metals to Chromium-Doped α-Al_2O_3

The fact that Cr_2O_3 and Al_2O_3 are isostructural and have very similar lattice parameters[1] (Table I) allows the preparation of solid solutions with a wide range of compositions.[2,3] This makes the $(Al,Cr)_2O_3$ system ideal for probing the effect of electron accepting dopants in the oxide phase on the strength of the interface. Preliminary adhesion energy measurements seem to indicate that the effect of chromium is that of enhancing adhesion.[4]

Our theoretical investigation of the effects induced on the adhesive properties by doping the oxide phase with chromium will start with a very simple model, adhesion of transition metals to the Cr_2O_3 (0001)O face. Later we will examine the variation of adhesion energy with dopant concentration. We will employ the slab models used elsewhere by us for the analysis of the adhesion of transition metals to the (0001)O surface of α-Al_2O_3,[5] replacing all aluminum atoms with chromium atoms. The models utilized contain the following features:

(a) A two-dimensionally periodic slab of both the oxide and the metal is used.

(b) The oxide slab is four oxygen and three aluminum layers thick, the metal slab is three layers thick.

(c) In the oxide layer we expose an oxide surface to the metal. The other oxide surface, away from the metal, is passivated by a hydrogen layer.

(d) The structures of the metal layers are modified slightly to provide epitaxy with the oxide.

A justification for these assumptions is provided in the study of Al_2O_3–metal interfaces.[5] The electron count is chosen to give charges of −2 on the oxygen atoms and +3 on all chromium atoms of the oxide phase. Note also that the parameters used in the extended Hückel calculations (see Appendix) for Cr^{3+} differ from those used to describe the metallic chromium layer, since the chemical character of both sites, ionic or metallic, is very different. Adhesion energy values are obtained by performing three separate calculations: one for each isolated component slab and another for the joint system. Adhesion energy is defined as $E_{adh} = E_{M/Ox} - (E_M + E_{Ox})$. Negative values thus imply stable interfaces.

Adhesion of transition metals to the (0001)O surface of α-Al_2O_3 was found to be dominated by M–O repulsive interactions at the surface.[5] Adhesion energies are calculated as repulsive for all first-row transition metals, except for scandium and titanium. 1 shows a schematic representation of the interactions at the Al_2O_3–metal interface. The upper band, mainly centered on the metal slab, is destabilized by interaction, giving a M–O antibonding interface band. Filling this band by electrons

Table I. Structural Parameters for Al_2O_3 and Cr_2O_3 in the Corundum Structure[a]

oxide	a	c	z (M)	x (O)
Al_2O_3	4.7589	12.991	0.3520	0.3060
Cr_2O_3	4.9607	13.599	0.3475	0.3060

[a] a and c are the lattice parameters (in Å) for the hexagonal unit cell. Metal cations are located at $\pm\{0,0,z\}$ and $\pm\{0,0,1/2+z\}$, oxygen atoms at $\pm\{x,0,1/4\}$, $\pm\{0,x,1/4\}$ and $\pm\{-x,-x,1/4\}$.

† On leave from the Departament de Química Física, Universitat de Barcelona, Barcelona, Catalunya, Spain.

(1) Newham, R. E.; De Haan, Y. M. Z. *Kristallogr.* **1962**, *117*, 235–237.
(2) Roy, D. M.; Barks, R. E. *Nature: Phys. Sci.* **1972**, *235*, 118–119.
(3) Graham, J. *J. Phys. Chem. Solids* **1960**, *17*, 18–25.
(4) Burlitch, J. M.; DeMott, G. J.; Kohlstedt, D. L. *Chem. Perspectives Electron. Mater.* **1989**, 453–8.
(5) Alemany, P.; Boorse, R. S.; Burlitch, J. M.; Hoffmann, R., submitted for publication.

0897-4756/93/2805-0465$04.00/0

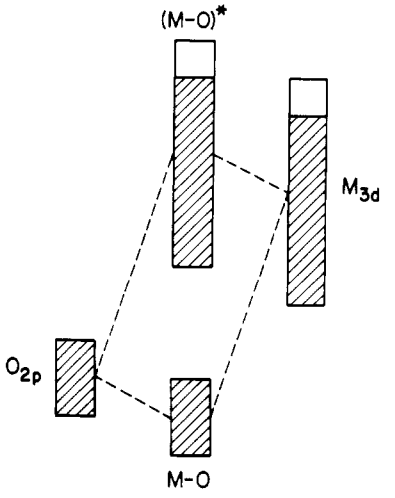

1

(moving from left to right across the transition metal series) will result in a weaker interface.

Keeping these results in mind, let us begin with the Cr_2O_3//Cr interface. How does the replacement of aluminum by chromium affect the basic interaction picture that we have established for α-Al_2O_3? The first difference is apparent when we compare the computed adhesion energy in both cases. Adhesion energies are calculated to be 0.65 and −29.31 J/m^2 for Al_2O_3 and Cr_2O_3 respectively. For the case of chromium oxide the sign of the adhesion energy is reversed, indicating that in this case the formation of the interface stabilizes the whole system. This value is excessively large; between 5- and 10-fold larger than might be plausibly expected. This behavior can be ascribed to the overestimation of charge transfer in one-electron calculations such as the extended Hückel method. Nevertheless, we think that trends are reproduced quite well by the method. The other quantity used to prove the adhesion strength, the O–M overlap population at the interface, has also increased from 0.221 in the case of α-Al_2O_3 to 0.293 for Cr_2O_3. Thus the net effect of replacing aluminum by chromium is enhanced adhesion of the modified oxide to the metal layer.

Examining the electronic structure of the Cr_2O_3 slab (Figure 1a), we find the O_{2p} band located at almost the same position as for α-Al_2O_3. The new features introduced in the density of states curve upon replacing aluminum with chromium are the bands extending from −10.5 to −9.5 eV and from −8.2 to −3.0 eV. These bands are derived from the t_{2g} and the e_g levels of the octahedrally coordinated chromium atoms. For the case of Cr^{3+}, a d^3 electron count results in a half filled t_{2g} band and an empty e_g band. Notice that the orbitals forming the t_{2g} band are formally Cr–O nonbonding orbitals centered mainly on the chromium atoms and will thus not be involved in direct interactions with the metallic layer across the interface.

What happens when we put the metal and the oxide together? The DOS curve obtained for the composite is very similar to the one obtained for the case of α-Al_2O_3, with the addition of the t_{2g} and the e_g bands mentioned above. The shaded area shown in Figure 1b is the contribution to the total DOS of the chromium atoms in the oxide. Comparison of this and the DOS for the isolated Cr_2O_3 layer shows that both the t_{2g} and the e_g bands remain almost unchanged upon interface formation, reflecting poor interaction with the metal. The t_{2g} band of the oxide

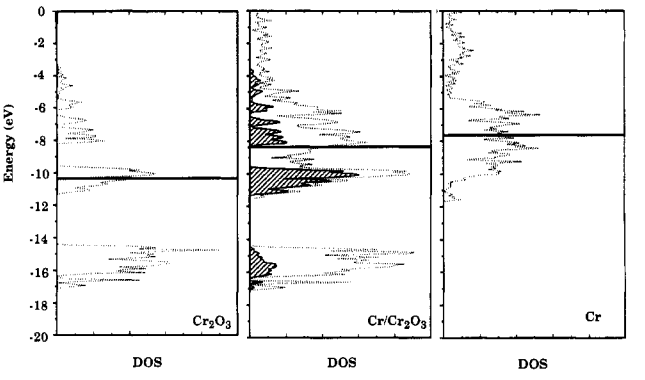

Figure 1. DOS curves for (a) the (0001)O surface of Cr_2O_3, (b) the Cr_2O_3-chromium interface, and (c) the chromium (110) surface. The shaded area indicates the Cr levels of the oxide face and the solid line indicates the Fermi level in each plot.

acts as an electron acceptor, as it lies lower in energy than the Fermi level of the isolated metal slab.

Addition of the t_{2g} band to the simple model described schematically by 1 leads us to a new model for the interaction of the doped ceramic with the metal slab. We see in 2 that, although the basic interactions are essentially

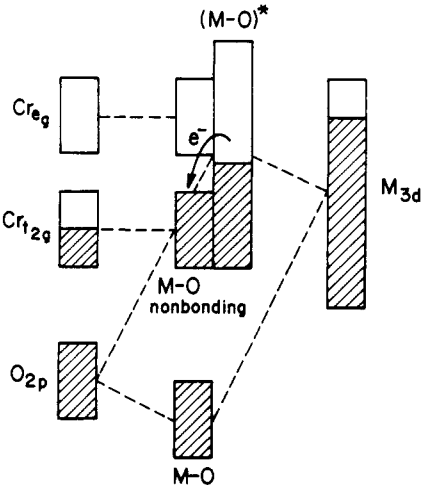

2

the same as those for α-Al_2O_3, the electron accepting band in the oxide is used by the metal to transfer part of its electrons, in this way lowering the energy of the whole system. It is also interesting to observe that the t_{2g} band is nonbonding with respect to the interface, so that the electrons are being transferred from formally metal–ceramic antibonding levels into a metal–ceramic nonbonding band, increasing the overlap population. This electron transfer is in good agreement with recent work by Li, in which the correlation between experimentally obtained work of adhesion values for metal–ceramic couples and the electron density of the metal as well as the thermodnamic stability of the oxide was demonstrated.[6] This correlation is explained in terms of charge transfer from the metal to the oxide.

Let us analyze the changes observed with variation of the metallic surface. In 3, a superposition of the t_{2g} bandwidth and the width of the d band for the different metals is shown. The Fermi levels of both subsystems are also indicated in 3. It can be concluded from this general

(6) Li, J.-G. *J. Am. Ceram. Soc.* **1992**, *75*, 3118–26.

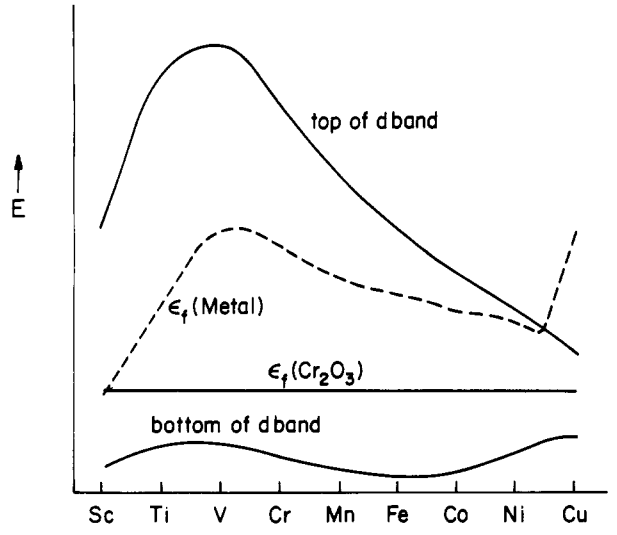

3

scheme that when replacing Al for Cr, no appreciable adhesion enhancement should be found for scandium. Adhesion enhancement should increase on moving to titanium and vanadium, reflecting the increase in energy of the Fermi level of these metals relative to the Fermi level of chromium oxide. On moving further across the first transition metal series, adhesion enhancement should decrease monotonically in magnitude to reach a minimum for nickel. A slight improvement due to the extra s electron, should be expected for copper, the last metal of the series. Figure 2a shows adhesion energies of interfaces of different metals for the α-Al_2O_3 (0001)O and Cr_2O_3 (0001)O surfaces. We can see that, in the case of chromium oxide, adhesion energies follow the predicted trend, nicely reflecting the variation of the position of the Fermi level for the different metallic slabs.

A comparison of the M–O overlap populations across the interface, Figure 2b, for α-Al_2O_3 and Cr_2O_3, reflects that both curves show the same trend; decreasing from left to right in the periodic table. The main difference is in magnitude, which is significantly larger for the case of chromium oxide. The curves are similar for two reasons: The number of accepting states in the t_{2g} band is fixed, implying that the number of metal–ceramic antibonding orbitals emptied by electron transfer is approximately constant through the series, and the t_{2g} band is noninteracting in nature.

Let us look now more closely at the effects induced in both slabs upon interface formation. Figure 3 shows the electron distribution of bulk and surface layers for the separated metal slabs. A detailed description of the charge balance between bulk and surface layers for metals has been given elsewhere[7-14] and will be reviewed only briefly here: 4 and 5 show schematically how the relative electron populations between bulk and surface layers are dictated by the different band widths of surface and bulk bands. For low fillings, bulk layers will be more populated than surface layers, while the opposite holds for almost filled bands. The differences in band width of bulk and surface bands arise from the fact that atoms on the surface have

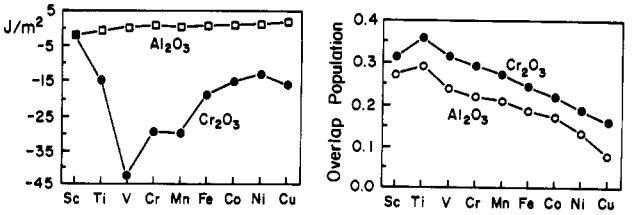

Figure 2. Adhesion energy (left) and interface overlap populations (right) for the interfaces formed with the Al_2O_3 and Cr_2O_3 (0001)O surfaces.

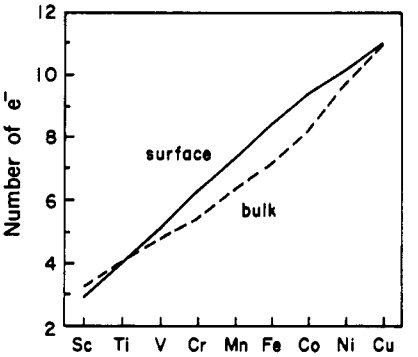

Figure 3. Relative charges for the surface and bulklike layers of the isolated metal slabs.

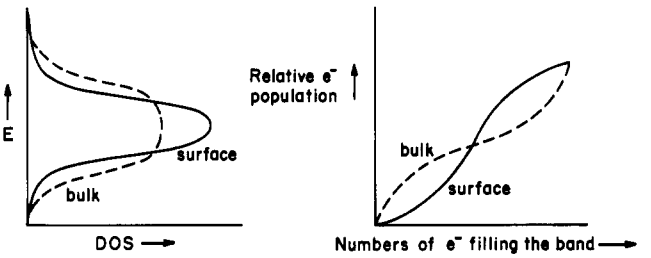

4 5

fewer neighbors. The less overlap atomic orbitals have with the neighboring atoms, the narrower the bands are.

Our actual calculations (Figure 3) show the same basic features as 5, although some differences appear because of changes in band energies and band widths that were not considered in the rigid band model used to derive 4 and 5.

To analyze the changes induced by the proximity of the oxide slab we may use arguments similar to those shown in 4 and 5. Interaction with the oxide slab will be stronger for the metal surface layer than for the bulk layers. This is reflected in a pushing up of the suface DOS with respect to the bulk DOS. The net effect of filling the band (moving from Sc to Cu) will be that of displacing the crossing point of 5 to the right, as shown in 6.

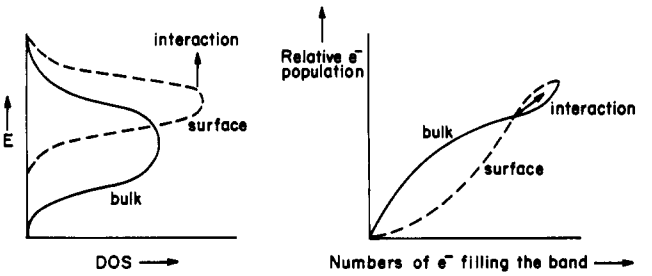

6

This is exactly what is observed for the case of α-Al_2O_3 (Figure 4a, top), although a more complicated model,

(7) Baetzold, R. *J. Am. Chem. Soc.* **1983**, *105*, 4271–4276.
(8) Desjonquères, M. C.; Spanjaard, D.; Lassailly, Y.; Guillot, C. *Solid State Commun.* **1980**, *34*, 807–810.
(9) Desjonquères, M, C,; Cyrot-Lackmann, F. G. *J. Chem. Phys.* **1976**, *64*, 3707–3715.
(10) Shustorovich, E. *J. Am. Chem. Soc.* **1980**, *102*, 5989–5993.

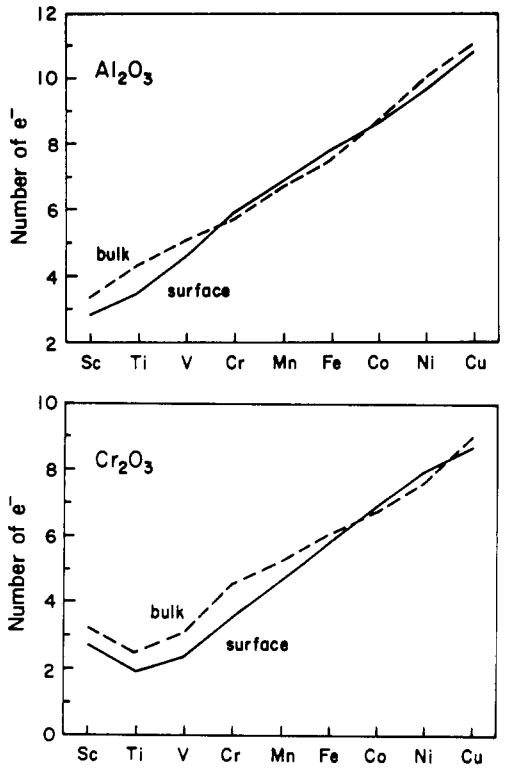

Figure 4. Relative charges for the surface and bulklike layers of the metal slabs for the metal–ceramic couples.

taking into account the different band width of each metal slab, would be required to explain the second crossing of both curves. In the case of Cr_2O_3, transfer of three electrons from the metal into the partially filled t_{2g} band of the oxide should result in a displacement of the crossing point by approximately three elements to the right of the transition series. This prediction is based on the assumption that substitution of chromium for aluminum does not alter the magnitude of the interaction between both surface layers. In Figure 4, bottom we see that our predictions are correct; the crossing point has been displaced from chromium to cobalt. This curve also reflects the fact that there is no possible charge transfer for the case of scandium (see 3).

To analyze the charge redistribution that takes place in the oxide slab we will use a slightly different method, focusing our attention on the change in slab charge upon forming the interface. The results are displayed in Figure 5. Positive values indicate that electrons have been transferred to the layer with interface formation, while negative values indicate electrons being donated by the layer.

From Figure 5a we can see that the surface oxygen layer of α-Al_2O_3 donates electrons. This is a small effect, decreasing from scandium to copper. The bulk layers, on the other hand, are hardly affected by the perturbation. A very different picture is obtained for the oxygen layers in Cr_2O_3 (Figure 5c). While the changes in the surface layer are similar (in magnitude and in trend), we see that there is electron accumulation in the bulk oxygen layers. This electron excess is approximately constant for the whole series (except for scandium, where no electron

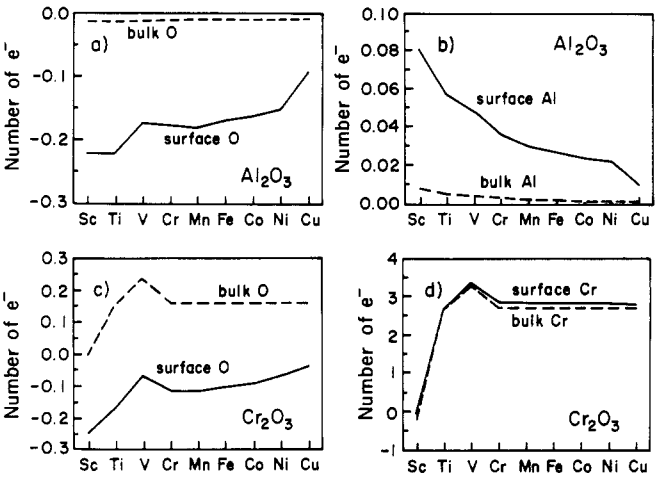

Figure 5. Charge changes in the oxide phase upon formation of the interface for (a) the oxygen atoms in Al_2O_3, (b) aluminum atoms in Al_2O_3, (c) oxygen atoms in Cr_2O_3, and (d) chromium atoms in Cr_2O_3.

transfer is possible). The exception of vanadium, ascribed to extra electron transfer that is possible only for this metallic slab, will be discussed later. The bulk oxygen atoms receive a small amount of charge—although the accepting t_{2g} band of the oxide is mostly centered on the chromium ions, there is some contribution of the surrounding oxygen atoms to this band. Charge transfer to this band will thus result in an increase of the charge on oxygen atoms.

Moving to the changes experienced by the cations, Figure 5b shows the results for aluminum ions in α-Al_2O_3, where the surface layer refers to the second layer of the slab. We can see that the changes are very small (notice the different scale on the figure) and are appreciable only in the surface layer. Bulk layers do not feel the presence of the metallic slab on the surface. Again, a very different picture is obtained for Cr_2O_3 (Figure 5d). We see that for almost all metals there has been a transfer of three electrons, filling the t_{2g} band, with the same exceptions to this general behavior; scandium with no charge transfer and vanadium. In the case of vanadium some extra electrons have been transferred, filling the bottom of the high-energy e_g band of the oxide. This effect depends on the parameters in our calculations, and we believe that transfer to a strongly antibonding band such as the e_g band is unlikely in any real system. The maximum in the Fermi level (see 3), makes vanadium the most likely candidate for this anomaly.

Although one can obtain good adhesion energies and strong bonds across the interface for a given system, this does not guarantee that both components will hold together. It is well-known that the flow of electrons created by formation of the interface is not innocent with respect to bonding inside the interacting systems. A very clear example of this may be found in surface-adsorbate interactions. Metal–adsorbate bonding is accomplished at the expense of bonding within the metal and the adsorbed molecule.[15] This effect is especially apparent in the case of dissociative chemisorption, where it leads to a breaking up of the adsorbed molecule. It has already been suggested that adhesive failure in the metal phase of a metal–ceramic couple can be as important as failure

(11) Shustorovich, E. *J. Phys. Chem.* **1982**, *86*, 3114–3120.
(12) Shustorovich, E. *Solid State Commun.* **1982**, *44*, 567–572.
(13) Shustorovich, E. *J. Phys. Chem.* **1983**, *87*, 14–17.
(14) Shustorovich, E.; Baetzold, R.; Mutterties, E. L. *J. Phys. Chem.* **1983**, *87*, 1100–1113.
(15) Hoffmann, R. *Solids and Surfaces: A Chemist's View of Bonding in Extended Structures*; VCH Publishers: New York, 1988.

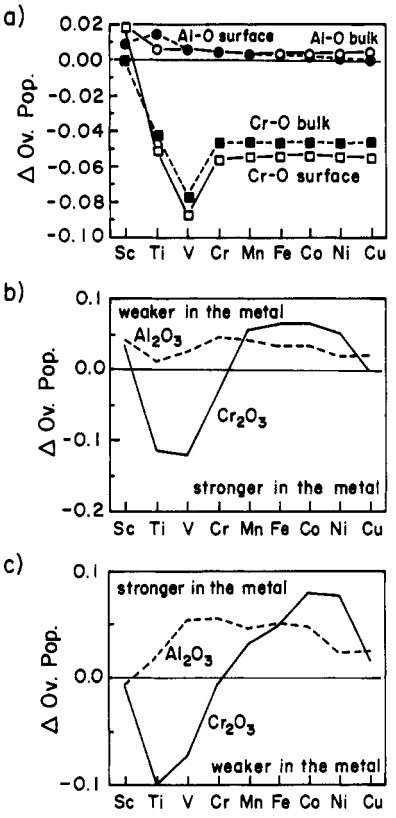

Figure 6. Changes in overlap populations upon forming the interface (a) for the oxides, (b) for the surface M–M bonds, and (c) for the surface–bulk M–M bonds.

of the interface itself.[16] It is also evident that failure in the oxide can play an equally important role in the mechanical characteristics of the total system.

Changes in overlap populations upon interaction are used to explore the possibility of adhesive failure in the metal or the oxide components. Although convenient for comparing the relative weakening of the components with changes in the metal, these quantities cannot be used as an absolute measure of the interfacial strength. Neither do they allow us to decide if a certain weakening of bonding on interface formation will lead to a decomposition of one or both components. They do allow us to say, for instance, that bonds in the oxide are stronger when the interface is formed with scandium than when it is formed with chromium.

The results obtained for the oxide component are displayed in Figure 6a. We can see that interaction with the metal has a small reinforcing effect on the Al–O bonds of α-Al_2O_3. For Cr_2O_3, electron transfer to the t_{2g} band, which is slightly Cr–O antibonding, weakens the bonds in the oxide approximately the same for all metals. The exceptions are scandium, where there is no effect due to the lack of charge transfer, and vanadium, where transfer to the highly antibonding e_g band results in a severe weakening of bonds in the oxide. Figure 6a shows that there are no important differences in the effects induced on the bonds between the first layer cations and the surface oxygen atoms and on the bonds between the first layer of cations and the bulk oxygen layer.

Parts b and c of Figure 6 show the differences in overlap population for the M–M bonds in the surface layer and between the surface layer and the inner layer, respectively.

(16) Nath, K.; Anderson, A. B. *Phys. Rev. B* **1989**, *39*, 1013–1019.

We can see that both types of bonds behave similarly. In both cases interaction with α-Al_2O_3 enhances the bonding inside the metal while interaction with Cr_2O_3 is more complex. For the early transition metals, M–M bonds are weakened, both in the surface and between surface and bulk layers. For the late transiton elements we find just the opposite situation: bonds are reinforced. This is due to two opposing factors in forming the interface. On one hand, mixing of oxide orbitals into the metal bands weakens the bonds in the metal phase. On the other hand, transfer of electrons into the t_{2g} acceptor band will result in a weakening for the early transition metals (most of the transferred electrons come from metal–metal bonding orbitals), and a reinforcement of metal–metal bonds for the late transition metals (where the transferred electrons are mostly metal–metal antibonding). For weak interaction with (0001)O surfaces, the second factor dominates, giving rise to the behavior observed in Figure 6.

From all the results obtained, chromium seems to represent the optimum metal for adhesion to Cr_2O_3. While it shows moderate adhesion strength at the interface, there is no bond weakening in the metal phase. Early transition-metal elements are more likely to show adhesive failure in the metal phase, while late transition elements are likely to form poor interfaces.

Effect of the Dopant Concentration on Adhesion Enhancement

The last part of this section will be devoted to the influence of dopant concentration on the adhesive properties of the $(Al,Cr)_2O_3$ system. The model used for this purpose is based on the same geometry as that used to model α-Al_2O_3 and Cr_2O_3. The unit cell contains six different cation sites, allowing us to calculate properties for oxides with dopant concentrations of Cr/(Cr + Al) = 0, $^1/_6$, $^1/_3$, $^1/_2$, $^2/_3$, $^5/_6$, and 1. Standard deviations for the calculated adhesion energies for a given concentration of dopant in different positions are approximately 0.5 J/m^2, indicating that the adhesion energy values do not depend strongly on the location of the dopant centers. This makes it possible for us to use the adhesion energy averaged over the different positional choices for each composition. While Cr doping in real α-Al_2O_3 is assumed to be random, the two-dimensional periodicity of the unit cell in our calculations does not produce a truly random model. The change in adhesion energies introduced by the translational periodicity of our model is anticipated to be small and relatively constant.

As we have seen, adhesion enhancement is obtained upon replacing aluminum by chromium due to the existence of a partially filled t_{2g} band that can act as an electron acceptor. From our previous results, we concluded that this band was not directly involved in interactions with the metal slab and that the mechanism of adhesion was based on electron dumping from the metal d band into the empty t_{2g} levels. The dependence of adhesion energy on concentration should be approximately linear (dashed line in Figure 7). More chromium atoms in the oxide will create more acceptor t_{2g}-type levels; this should enhance the adhesion energy.

Figure 7 shows that this linear dependence is valid only for low concentrations of dopant atoms. Chromium concentrations greater than $x_{Cr} = 0.2$ show a clear deviation from linear behavior and are calculated to be weaker than expected from the simple model of a rigid acceptor band.

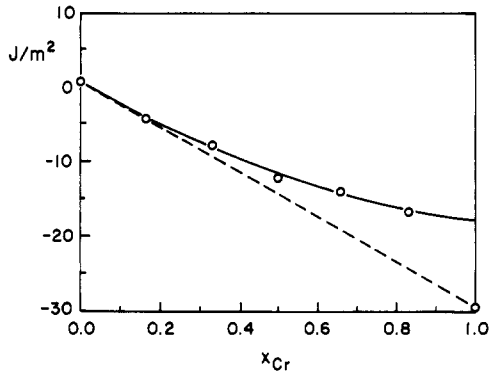

Figure 7. Adhesion energy for $(Al,Cr)_2O_3$–chromium interfaces with different chromium content in the oxide. The dashed line represents the case of a perfectly noninteracting acceptor band.

Where do these differences come from? The basic assumption of the model, that the metal slab is interacting only with the O_{2p} band, and that the t_{2g} band of chromium oxide is not involved in the interaction and is acting merely as an electron acceptor, is no longer true for intermediate compositions. This is illustrated clearly in **7**, where the

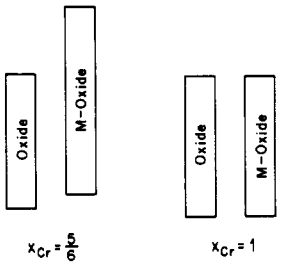

7

position of the t_{2g} band before and after interaction with the metal slab is shown, for both Cr_2O_3 and an intermediate composition. The t_{2g} band remains pratically unchanged in the case of Cr_2O_3, but interaction with the slab pushes the band up in energy for the intermediate composition. That the interaction with the metal slab results in a destabilization of the t_{2g} band explains why the calculated values for the adhesion energy are lower than expected for the rigid t_{2g}-band model. While the number of electrons dumped follows a linear relationship with the concentration, this in not the case with the energy gain per transferred electron.

With intermediate compositions, the lack of d orbitals on some of cationic sites results in a larger oxygen contribution in the t_{2g} band, increasing the interaction of this band with the metallic slab. This results in a net reduction of the predicted adhesion energies.

A few remarks need be made to conclude the discussion on the effect of doping. In the model used for this study, important effects have been neglected that will modify the adhesive properties. The clearest indication of this is in the large values obtained for the adhesion energies. The t_{2g} set of orbitals, mainly centered on the chromium atoms, has poor overlap with the neighboring atoms, thus giving a relatively narrow band. Electrons in this band will be strongly localized, a situation in which electron–electron repulsion effects may be important. Our one-electron model does not take into account the repulsive energy that will be experienced by the electrons dumped into the partially filled t_{2g} band. A transfer of three electrons per dopant atom, as obtained in our calculations, is surely too large. Electron–electron repulsion will play an important role in this case, lowering the actual amount of charge transfer, and thus, the adhesion energy.

It is easy to see that our method overestimates charge transfer. In the case of a perfectly noninteracting acceptor band, the difference in Fermi levels of both the metal and the oxide slab will result in an electron flow even if both slabs are at infinite separation! The reason for this unphysical situation is the neglect of electron–electron interaction in our method. A simple electrostatic argument indicates that for each electron transferred to the oxide, the accumulation of negative charge in this phase will make it more difficult to transfer the next electron. The net effect is that fewer electrons are transferred, until the energy gained by dumping electrons from a high-lying to a low-lying band is insufficient to compensate for the electron repulsion in the low-lying oxide band. It is quite difficult to make even a crude approximation of the magnitude of these effects. Although there have been attempts to obtain qualitative estimates of interelectronic effects from experimental data, these are known only for a limited number of cases and the results obtained are of poor quality. On the other hand, ab initio inclusion of these effects in the quantum mechanical model for complex systems such as interfaces lies for the moment out of reach. However, quickly developing theoretical tools based on density functional theory may change this.[17,18]

Table II. Extended Hückel Parameters

atom	orbital	H_{ii} (eV)	ξ_1	ξ_2	c_1	c_2
Al[28]	3s	−12.30	1.17			
	3p	− 6.50	1.17			
O[23]	2s	−32.30	2.28			
	2p	−14.80	2.28			
Sc	4s	− 5.70	1.30			
	4p	− 2.94	1.30			
	3d	− 9.50	4.35	1.70	0.4228	0.7276
Ti	4s	− 6.30	1.50			
	4p	− 3.20	1.50			
	3d	− 8.00	4.55	1.40	0.4206	0.7839
V[29]	4s	− 6.70	1.60			
	4p	− 3.40	1.60			
	3d	− 6.70	4.75	1.50	0.4560	0.7520
Cr[29]	4s	− 7.30	1.70			
	4p	− 3.60	1.70			
	3d	− 7.90	4.95	1.60	0.4876	0.7205
Mn[29]	4s	− 7.50	1.80			
	4p	− 3.80	1.80			
	3d	− 8.70	5.15	1.70	0.5140	0.6930
Fe[29]	4s	− 7.60	1.90			
	4p	− 3.80	1.90			
	3d	− 9.20	5.35	1.80	0.5366	0.6678
Co[29]	4s	− 7.80	2.00			
	4p	− 3.80	2.00			
	3d	− 9.70	5.55	1.90	0.5550	0.6678
Ni[29]	4s	− 7.80	2.10			
	4p	− 3.70	2.10			
	3d	− 9.90	5.75	2.00	0.5683	0.6292
Cu	4s	− 7.80	2.20			
	4p	− 3.46	2.20			
	3d	−10.00	5.95	2.30	0.5933	0.5744
H[23]	1s	−13.60	1.30			
(Cr^{3+})[30]	4s	− 8.66	1.70			
	4p	− 5.24	1.70			
	3d	−11.22	4.95	1.60	0.5060	0.6750

Conclusions

Our results suggest that doping of α-Al_2O_3 with transition-metal cations should enhance the adhesive prop-

(17) Ziegler, T. *Chem. Rev.* **1991**, *91*, 651–667.
(18) Jones, R. O.; Gunnarson, O. *Rev. Mod. Phys.* **1989**, *61*, 689.

Table III. Structure, Interacting Faces, and Interlayer Distances (Å) for the Metallic Slabs Used in the Calculations

M	Sc	Ti	V	Cr	Mn	Fe	Co	Ni	Cu
struct	hex	hex	bcc	bcc	bcc	bcc	hex	fcc	fcc
face	(0001)	(0001)	(110)	(110)	(110)	(110)	(0001)	(111)	(111)
d_{M-M}	2.63	2.34	2.14	2.04	2.18	2.07	2.03	2.03	2.08

erties between alumina and metal surfaces. There are experimental reasons for the use of chromium as a dopant (easy formation of solid solutions with a large range of different compositions). From the preceding discussion, the adhesion energy is enhanced by accepting properties of the partially filled t_{2g} band of the dopant centers. If it would be possible to have dopants providing more acceptor levels (e.g., V^{3+}), adhesion should be enhanced. Another way to achieve this goal would be to lower the energy of the t_{2g} band, replacing chromium by some transition metal on the right part of the transition metal series. It is however difficult to predict which of two effects—low occupancy of the t_{2g} band (moving to the left in the transition-metal series), or lowering the energy of the t_{2g} band (moving to the right)—would dominate.

Acknowledgment. The stay of P.A. at Cornell University has been made possible through a postdoctoral grant of the Ministerio de Educación y Ciencia of Spain. P.A. is grateful to A. L. Tchougreeff for his critical comments during the realization of this work. The authors also would like to thank Jane Jorgensen for the drawings. Our work at Cornell was supported by the National Science Foundation, through the Materials Research Center, Research Grant DMR-9121654. This research was conducted using the resources of the Cornell Theory Center, which receives major funding from the National Science Foundation and IBM Corp., with additional support from New York State Science and Technology Foundation and members of the Corporate Research Institute.

Appendix

All calculations presented in this paper have been performed using the tight-binding formalism[19-21] within an extended Hückel[22,23] framework. The atomic parameters used in the calculations are listed in Table II. A set of 30 k points in the 2D hexagonal Brillouin zone was used for the calculation of average properties on the (0001) type interfaces. This set of special k points was obtained using the geometric method described by Ramírez and Böhm.[24]

The α-Al_2O_3 experimental bulk geometry obtained from X-ray diffraction experiments[1,25] has been used for the oxide phases (Table II). Table III indicates the exposed faces and the interlayer distances[26] chosen in the calculations for the metals. The stacking pattern of the three modified layers included in the metal models follows the original structure of the metal. An interface distance of 2.0 Å has been used in all calculations in order to simplify comparison of results. M–O distances for the first transition-metal series average somewhat less than 2.0 Å for discrete complexes, for example, Cr–O = 1.79 Å for $Cr_2O_7^{2-}$ [27] and show a great range usually exceeding 2.0 Å for solid-state oxides, for example, Co–O = 3.29 Å for Co_3O_4[26] but Ni–O = 2.05 Å for NiO.[26] No important differences in the basic interactions are expected if this interlayer distance were changed within reason.

(19) Ashcroft, N. W.; Mermin, N. D. *Solid State Physics*; Holt, Rinehart and Winston: New York, 1976.
(20) Whangbo, M.-H.; Hoffmann, R. *J. Am. Chem. Soc.* **1978**, *100*, 6093.
(21) Whangbo, M.-H.; Hoffmann, R.; Woodward, R. B. *Proc. R. Soc. London, A* **1979**, *366*, 23.
(22) Hoffmann, R.; Lipscomb, W. N. *J. Chem. Phys.* **1962**, *36*, 2176–2195.
(23) Hoffmann, R. *J. Chem. Phys.* **1963**, *39*, 1397–1412.
(24) Ramírez, R.; Böhm, M. C. *Int. J. Quantum Chem.* **1986**, *30*, 391.
(25) Pauling, L.; Hendricks, S. B. *J. Am. Chem. Soc.* **1925**, *47*, 781–790.
(26) Pearson, W. B. *Handbook of Lattice Spacings of Metals and Alloys*; Pergamon: New York, 1958.
(27) Greenwood, N. N.; Earnshaw, A. *Chemistry of the Elements*; Pergamon Press: New York, 1984.
(28) Anderson, A. B.; Hoffmann, R. *J. Chem. Phys.* **1974**, *60*, 4271.
(29) Saillard, J.-Y.; Hoffmann, R. *J. Am. Chem. Soc.* **1984**, *106*, 2006–2026.
(30) Summerville, R. H.; Hoffmann, R. *J. Am. Chem. Soc.* **1976**, *98*, 7240.